Journal of Thermal Analysis and Calorimetry, Vol. 92 (2008) 1, 331–335

ROMAN CERAMICS OF HYDRAULIC MORTARS USED TO BUILD THE MITHRAEUM HOUSE OF MÉRIDA (SPAIN)

M. L. Franquelo[1], *M. D. Robador*[2], *V. Ramírez-Valle*[1], *A. Durán*[1], *M. C. Jiménez de Haro*[1] *and J. L. Pérez-Rodríguez*[1*]

[1]Institute of Materials Science of Sevilla, CSIC-Sevilla University, Américo Vespucio s/n 41092 Sevilla, Spain
[2]Faculty of Technical Architecture, Sevilla University, Avda. Reina Mercedes s/n, Sevilla, Spain

Roman ceramics of two hydraulic mortars used to build the pond and water channel of Mithraeum house from Mérida (Spain) have been studied. The sizes of the ceramic fragments found were different in both of the samples studied, showing different behaviour in the reactions with the lime. The X-ray diffraction of the ceramic shows the presence of quartz, mica (biotite), anorthite and hematite accompanied by amorphous phase, being observed scarce vitrification. The presence of mica confirms a firing temperature for manufacturing the ceramic below 900°C. In one of the ceramics studied, X-ray diffraction did not show calcite. However, in the FTIR appear bands that could be assigned to carbonates absorptions and likewise, carbonates were identified in the DTA-TG curves. Ca and small quantities of Si and Al were also identified by SEM-EDX on the surface of the pores that could be due to an amorphous phase formed in the reaction of lime with the Si and Al of the ceramic. On the other hand, in other ceramic samples carbonates (about 10%) were detected. The carbonates have been found filling the pores, sometimes accompanied by a new calcium–aluminium–silicate phase produced by the reaction between the lime and the amorphous phase of the ceramic. The carbonates and the new phases formed inside the pores are responsible for the decrease of the porosity and for the formation of new phases during the heating of the ceramics.

Keywords: *carbonates, ceramic, firing temperature, lime reactions, mortars, porosity*

Introduction

The characterization of ancient mortars provides useful information about how low complex architectural structures were realised [1–4]. Lime was used in the antiquity as non-hydraulic cement mixed with pozzolanes specially to build duct drains, cisterns and swimming pools [5, 6].

The hydraulic compounds (those with the property of hardening when water is added to the dry binder, and also the capacity of growing harder under water) are obtained from the reactions of $Ca(OH)_2$ with natural pozzolanes (natural earth of volcanic source) or artificial ones (such as ground fired bricks and tiles or ceramic shreds). In ceramic materials obtained from kaolinite, a very reactive amorphous aluminium silicate is present. The presence of aluminium and iron oxides together with the lime binder contributes to the mortar hydraulic character [7–12].

Roman mortars and ceramics have been widely studied [13, 14], while less attention has been paid to the ceramic used for hydraulic mortars. The ceramic used requires high reactivity, which is obtained by heating between 600 and 800°C. The amorphous silica reacts with the lime used for making the mortar. The reaction degrees of alkalisilica reaction (ASR) were studied on crushed natural reactive aggregates kept in contact with alkaline solution (lime), which resulted in the breaking up of the siloxane bands, in the formation of $SiO^{-}_{5/2}$ sites and in their subsequent dissolution and/or inclusion into the internal silica gel [15, 16]. The dissolution of silica is due to the continued attack of hydroxide ions on the SiO_2 sites, to form silicate ions [17, 18].

The transformation of $Ca(OH)_2$ to $CaCO_3$ occurs through several intermediate compounds (hydrated gel of calcium silicate and aluminium, ion calcium silicate) being difficult their characterization by XRD due to their small proportion and amorphous character [19]. The aqueous solution of $Ca(OH)_2$ (1.6 g L^{-1}) reacts with the surface of the ceramic [20, 21]. Also small particles of $Ca(OH)_2$ may be introduced in the pores of the ceramic producing alteration of its surface.

The aim of this work implies the characterization of the ceramics used for roman mortars from Mithraeum house (Mérida, Spain) and the possible raw materials used for its manufacture. Additionally, the reactions between the surfaces of the ceramic and the lime of the mortar will be investigated.

* Author for correspondence: jlperez@icmse.csic.es

1388–6150/$20.00

Akadémiai Kiadó, Budapest, Hungary
Springer, Dordrecht, The Netherlands

Experimental

Materials

The roman house of Mithreaum in Mérida. Mérida, the Roman Augusta Emerita, was founded in the year 25 BC. The house must have been built in the last years of the Ist century AC, or at the beginning of the IInd century AC. The domus, by means of the patio pools, performs the collection of rainwater, which, via a network of channels, leads to the main cistern. Hydraulic mortar obtained with ceramic was employed in this house.

Samples were taken using hammer and chisel from the following parts of the building: pond of peristilo (Sample 1); water channel from viridarium (Sample 2). The ceramics of the mortars were separated with pliers.

Methods

The porosity of the mortars was determined using the UNE 83-820-94. EX procedure. The pH was measured using a pHmeter, Hanna meurtex model HI 8314. The proportion of lime/sand/ceramic was identified using the method proposed by Robador [22].

Differential thermal analysis and thermogravimetric analysis (TG) measurements were performed by means of a Seiko TG/DTA 6300 simultaneous analyser. X-ray diffraction diagrams (XRD) were obtained using a Siemens diffractometer model Kristallofex D-5000. Fourier transform infrared spectra were taken by a Nicolet 510 covering the 400–4000 cm^{-1} range. SEM investigation was performed by a Jeol JSM 5400 microscope equipped with an energy dispersive X-ray analyser (EDX). The porosity of the ceramic was evaluated by calculating the total area of the distribution curve obtained by mercury Quantachrome Poremaster porosimeter.

Results and discussion

Mortars

Both studied mortars have a high ceramic content (the proportions of lime/ceramic/sand are 1/1.8/1 and 1/1.5/1 for samples 1 and 2, respectively), giving them a high hydraulic property; the alkaline pH 7.5 shows that part of the calcium hydroxide has not been transformed in carbonate, probably due to the absence of contact between the mortar and the air. Sample 2 shows higher density and smaller porosity in comparison with sample 1.

The XRD diagram of the mortar after removing the ceramic fragments (Fig. 1a) shows quartz and calcite; in addition, mica and anorthite also appear.

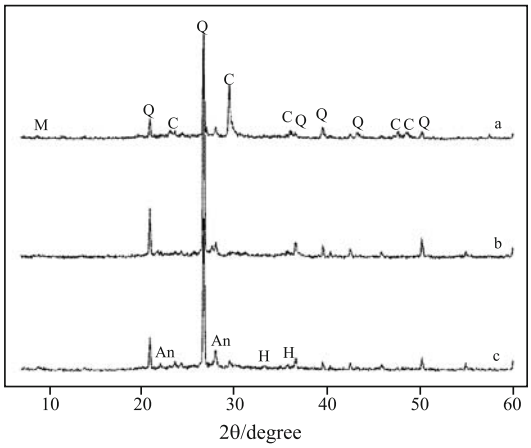

Fig. 1 XRD patterns of a – mortar, b – ceramic from sample 1, c – ceramic from sample 2. Q=quartz, C =calcite, H=hematite, M=mica, An=anorthite

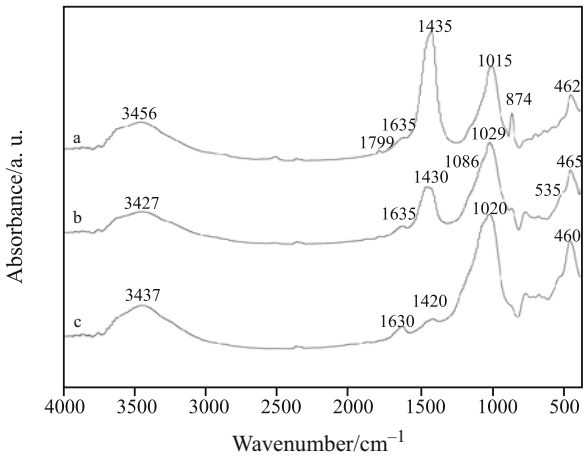

Fig. 2 IR spectra of a – mortar, b – ceramic from sample 2, c – ceramic from sample 1

The FTIR spectra of the mortar samples (Fig. 2a) show characteristic bands of carbonates (1799, 1435, 874 and 714 cm^{-1}), free hydroxyl ion of water (at about 3440 cm^{-1}) and silicates (1015 and 462 cm^{-1}).

Ceramics

The size of the ceramic fragments in sample 2 (from the water channel from the viridarium) was smaller (5 mm·3 mm·2 mm–1 mm·1 mm·0.5 mm) than the size of the ones taken from the peristilum (sample 1) (16×18×12 mm–6×5×5 mm). These different sizes could affect the interaction with the lime of the mortar.

The chemical analysis of both samples show similar composition with high proportion of SiO_2, Al_2O_3, Fe_2O_3 and MgO and K_2O to a lesser degree. These data suggest the use of aluminate and/or ironaluminate silicate for the manufacture of the ceramic. The sample 2 shows an increase of the CaO

from 2.48% (in sample 1) up to 4.42%, keeping similar percentages for the other chemical components.

The XRD diagram of the ceramic in sample 1 (Fig. 1b) shows the presence of quartz as main component; in addition, anorthite, hematite and mica also appear in small proportion. The study by XRD was also carried out in ten ceramic samples separated from the pond of the peristilo, all of them showing absence of calcite. In sample 2, constituted by smaller ceramic fragments, the XRD shows the presence of calcite together with quartz, anorthite and muscovite (Fig. 1c).

The microphotograph of the ceramic sample 1 observed by SEM (Fig. 3a) shows in the centre a stack of flakes constituted by Si, Al, Mg, K and Fe, according with the chemical analysis carried out by EDX. These data suggest that this particle is mica (biotite).

Some clay minerals are transformed in amorphous phase during heating. Kaolinite, transforms at 500°C into metakaolin; this amorphous phase remains in the sample up to very high temperature, being impossible to characterize it by XRD. Heating of metakaolin forms alumina-type spinel at 980°C and leads to mullite crystallization at higher temperature (about 1200°C) [23–30]. In order to determine if some amorphous phase remains in the ceramic, the samples were heated at high temperature.

The XRD diagram of the sample 1 heated at 1100°C during 2 h (fig. not shown) only shows a decrease of the intensity of the quartz diffractions, appearing ferrian spinel. The presence of ferrian spinel suggests the presence of mica biotite in the used clays [31]. After heating, peaks of small intensity at 3.42, 3.37, 2.54 and 2.21 also appear, suggesting the initial formation of mullite.

It is known that during the firing, clays decompose and react to form new microcrystalline mineral phases. The assemblage quartz+plagioclase+feldspar+ferrian spinel+illite (temperature range of 850–950°C) is the

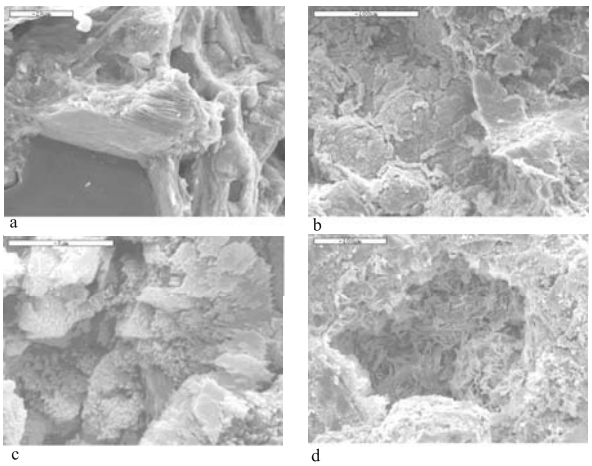

Fig. 3 SEM micrographs of a, b, c – ceramic from sample 1, d – ceramic from sample 2

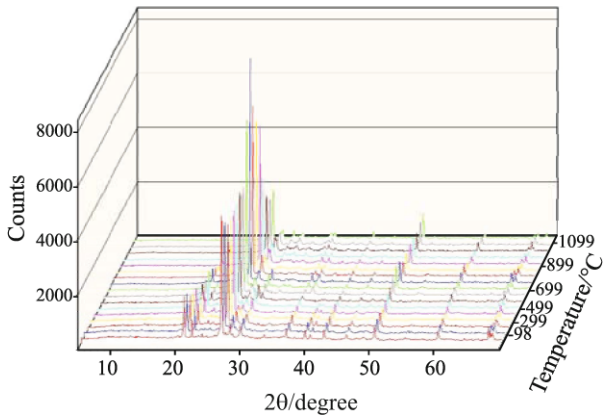

Fig. 4 XRD patterns of sample 2 heated between 30–1100°C

composition we have found by XRD in ceramics studied in this work.

The XRD diagrams of sample 2 (where calcite was detected) heated in a high temperature chamber from 30 to 1100°C at 10°C min^{-1} were registered every 50°C (Fig. 4). Some modifications of the diagrams appear during the heating process such as the decomposition of calcite between 600 and 650°C [32], appearing CaO that disappears at 850°C, probably due to the reaction with silica. The intensity of the quartz peak at 3.34 also decreases at 850°C.

FTIR spectra of samples 1 and 2 (Figs 2b and c) show bands of silicates and iron oxides. In sample 1, presence of carbonate was not detected by XRD, however the presence of this phase is suggested by a small band at 1420 cm^{-1}. In sample 2, the increase in the intensity of the band at 1430 cm^{-1} is attributed to a higher carbonate concentration.

The DTA curves (Fig. 5) show endothermic effects about 100°C (attributed to adsorbed water), 573°C ($\alpha \rightarrow \beta$ phase transformation of quartz) and about 750°C (carbonate decomposition). Relation between mass loss due to CO_2 (mass loss attributed to the carbonate decomposition between 600 and 900°C) and H_2O (mass loss attributed to the decomposition of chemically bound water of hydraulic products between 200 and 600°C) is used to determine the hydraulic character of the mortar. This relationship does not provide useful information in our study because the ceramic fragments have been separated from the mortar and, therefore, have only partially reacted with the lime.

The TG curves show mass losses between 30–200°C due to adsorbed water. The mass losses between 200–600°C corresponding to structural bound water, responsible from the hydraulic character of the mortar are 2.8 and 4.0% for samples 1 (Fig. 5b) and 2 (Fig. 5a), respectively. The higher mass losses due to structural bound water and decomposition of carbonate in sample 2 indicates a major extent in the

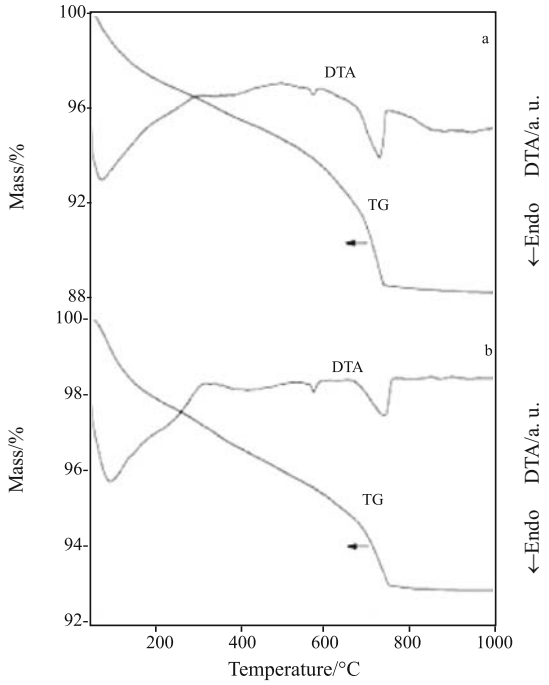

Fig. 5 DTA and TG of a – ceramic from sample 2; b – ceramic from sample 1

reaction between ceramic and lime. The previously described XRD diagrams did not show the presence of carbonates in sample 1, while the DTA and TG analysis confirmed that carbonates were present in the mentioned samples [33–35]. The mass losses between 600–750°C attributed to the decomposition of carbonate are 2.2 and 5.0% for samples 1 (Fig. 5b) and 2 (Fig. 5a), respectively.

More information about the present carbonates in the ceramic has been obtained using scanning electron microscopy. The SEM microphotograph of sample 1 (Fig. 3b) shows the characteristic surface of the ceramic, appearing different phases in the pores. Increasing the magnification we can observe the morphology of this phase (Fig. 3c). The microanalysis of this phase shows the presence of Ca.

In sample 2, this Ca phase also appears in high percentage, together with another phase constituted by Si, Al and Ca (Fig. 3d). These results show that the lime has penetrated inside the pores of the ceramic forming carbonates and reacting with the silicates.

The sample 1 shows higher porosity (with a bimodal distribution of high dispersion) than the sample 2 (with a monomodal distribution). This difference may be attributed to a higher penetration of lime inside and formation of carbonates and reaction products with the Si and Al of the ceramic in the sample 2.

Conclusions

Two types of aggregates have been recognized in the hydraulic mortars: crushed ceramics and sand. The found fragments of ceramics are smaller in sample 2 than in sample 1, this difference in size is responsible of their different behaviour in the interaction with the lime. The sand aggregates are constituted mainly by quartz; in addition, plagioclase, K-feldspar and mica appear.

Lime is used as binder, showing a heterogeneous composition due to calcite phases. Primary hydromorphic crystals and calcite micrograins of secondary crystallisation (partially amorphous) have been found.

Results of mineralogical analysis on ceramic fragments can provide information about maximum burning temperature used. The chemical analysis shows a high content of SiO_2 followed by Al_2O_3. The presence of Fe_2O_3, MgO, K_2O and CaO was also observed. The SEM-EDX together with XRD confirms the presence of quartz, mica (biotite), iron oxides, and anorthite in agreement with the data obtained by chemical analysis. These minerals were present in the raw material used to manufacture the ceramic together with other phases not detected, mainly constituted by Si and Al, i.e. kaolinite, which transforms in amorphous phase when heated about 500°C [36]. Above this temperature the total transformation of this phase occurs, appearing a transient alumina or alumina-type spinel forms at 980°C while mullite crystallization follows at higher temperature. This phase is not present in our samples. The presence of mica in these ceramics indicates that the firing temperature was lower than 900°C [37–39]. The microscopy study shows that vitrification is very scarce, but enough to start the formation of new phases. The heating of the ceramic (sample 1) at 1100°C shows peaks of low intensity in the XRD diagrams attributed to mullite. Also the muscovite or illite present in our samples may produce mullite. The chemical analysis carried out by EDX in different points shows the relation Si/Al between 2 and 3 in agreement with the presence of mica (biotite). Ferrian spinel is the phase clearly formed after the heating of the ceramic, suggesting that this phase could be formed from the destruction of biotite present in the ceramic studied in this work. In sample 2 the higher content of Ca may be responsible of some differences during the ceramic heating. The $CaCO_3$ is decomposed appearing peaks of CaO at 650°C. At higher temperature an increase of anorthite appears probably due to the reaction of the silicate with the present calcium compounds. The presence of K-feldspars in sample 2 was confirmed because the sample 2, unlike sample 1, fused when heated at 1100°C.

The mixture between the ceramic and the lime from the mortar produced reactions between both

materials. The ceramic fragments of the sample 1 are 3 times higher in comparison with those of sample 2. The differences in size of both samples may be responsible of different behaviour of both ceramics. Carbonates in low percentages are detected in sample 1 by FTIR and DTA-TG study. However carbonates are not found by XRD probably due to the low percentage present or to the amorphous character of the present phase as was described previously. In sample 2, calcite was detected in a percentage about 10%.

The scanning electron microscopy and chemical analysis carried out by EDX provides information of the interaction between the lime and the surface of the ceramic. Thus, in pores of sample 1 minerals of secondary calcite with a certain amount of SiO_2 and Al_2O_3 appear.

In sample 2 not only carbonates (like in sample 1) but a calcium aluminium silicate phase are found produced by reaction between lime and aluminium silicate mainly amorphous phase produced during the manufacture of the ceramic.

References

1 M. Franzini, L. Leoni, M. Lezzerini and F. Sartori. Eur. J. Mineral., 6 (2000) 1151.
2 A. Moropoulou, A. Bakolas and K. Bisbikou. J. Cult. Herit., 1 (2000) 45.
3 G. M. Crisci, M. Davoli, A. M. De Francesco, F. Gaghardi, P. Mercurio and D. Miriello, Arkos, 3 (2001) 36.
4 J. Pires and A. J. Cruz, J. Therm. Anal. Cal., 87 (2007) 411.
5 K. A. Harries, Concr. Int., 1 (1995) 58.
6 S. L. Marusin, Concr. Int., 1 (1996) 56.
7 A. Bakolas, G. Biscontin, V. Contardi, E. Franceschi, A. Moropoulo, D. Palazzi and E. Zendri, Termochim. Acta, 269/270 (1995) 817.
8 A. Moropoulou, A. Bakolas and K. Biskikou, Thermochim. Acta, 269/270 (1995) 779.
9 L. Poama, I. Pitkamen, H. Rönkkömäki and P. Periämäki, Thermochim. Acta, 320 (1998) 127.
10 J. I. Alvarez, I. Navarro and P. J. García Casado, Thermochim. Acta, 320 (1998) 127.
11 P. Maravelaki-Kalaitzaki, A. Moropoulou and A. Bakolas, Cem. Concr. Res., 33 (2003) 651.
12 A Moropoulou, A. Bakolas and K. Bisbikou, Thermochim. Acta, 269/270 (1995) 779.
13 J. Elsen. Coment Concr. Res., 36 (2006) 1416.
14 R. García Giménez, R. Vigil de la Villa, P. Recio de la Rosa, M. D. Petit, Domínguez and M. I. Rucandio, Talanta, 65 (2005) 86.
15 H. Wang and J. E. Gillot, Cem. Concr. Res., 21 (1991) 647.
16 D. Bulteel, E. García-Diaz, C. Vernet and H. Zanni, Cem. Concr. Res., 32 (2002) 1199.
17 J. Verstraete, L. Khouchaf, D. Bulteel, E. García-Díaz, A. M. Flank and M. H. H. Tuilier, Cem. Concr. Res., 344/4 (2004) 581.
18 R. K. Iler, The Chemistry of Silica, Wiley, New York 1979.
19 E. T. Stepkowska, M. A. Aviles, J. M. Blanes and J. L. Pérez-Rodríguez, J. Therm. Anal. Cal., 87 (2007) 189.
20 E. T. Stepkowska, J. L. Pérez-Rodríguez, M. J. Sayagues and J. M. Blanes, J. Therm. Anal. Cal., 73 (2003) 247.
21 E. T. Stepkowska, J. L. Pérez-Rodríguez, M. C. Jiménez de Haro and M. J. Sayagues, J. Therm. Anal. Cal., 69 (2002) 187.
22 D. Robador. Tesis Doctoral, Sevilla University (2000).
23 V. Balek, L. A. Pérez-Maqueda, J. Poyato, Z. Cerny, V. Ramírez-Valle, I. M. Buntseva and J. L. Pérez-Rodríguez, J. Therm. Anal. Cal., 88 (2007) 87.
24 L. A. Pérez-Maqueda, J. L. Pérez-Rodríguez, G. W. Scheiffele and P. J. Sánchez-Soto, J. Thermal Anal., 39 (1993) 1055.
25 P. J. Sánchez-Soto and J. L. Pérez-Rodríguez, J. Am. Cer. Soc., 72 (1989) 154.
26 P. J. Sánchez-Soto, I. Sobrados, J. Sanz and J. L. Pérez-Rodríguez, J. Am. Cer. Soc., 76 (1993) 3024.
27 S. J. G. Sousa and J. N. F. Holanda, J. Therm. Anal. Cal., 87 (2007) 115.
28 H. Connan, A. Rey, P. Thomas and J.-P. Guerbois, J. Therm. Anal. Cal., 87 (2007) 115.
29 F. Franco, L. A. Perez-Maqueda and J. L. Perez-Rodriguez, Thermochim. Acta, 404 (2003) 71.
30 J. L. Perez-Rodriguez, J. Pascual, F. Franco, M. C. J. de Haro, A. Duran, V. R. del Valle and L. A. Perez-Maqueda, J. Europ. Ceram. Soc., 26 (2006) 747.
31 M. M. Jordan, A. Boix, T. Sanfeliu and C. De la Fuente, App. Clay Sci., 14 (1999) 225.
32 L. A. Perez-Maqueda, A. Ortega and J. M. Criado, Thermochim. Acta, 277 (1996) 165.
33 T. L. Webb and J. E. Krüger, Differential Thermal Analysis, R. C. McKenzie, Ed., Academic Press. London and New York 1970. V. d.p. 1, 103 and V. d. 2, 181.
34 L. Paama, I. Pitkanen and P. Peramaki, Thermochim. Acta, 320 (1998) 127.
35 A. Bakolas, G. Biscontin, V. Contardi, A. Moropoulo and E. Zendri, Thermochim. Acta, 321 (1998) 151.
36 G. Brown and G. W. Brindley, Crystal Structures of Clay Minerals and their X-ray Identification, G. W. Brindley and G. Brown, Eds Mineralogical Society, London 1957, 305.
37 L. A. Pérez-Maqueda, J. M. Blanes, J. Pascual and J. L. Pérez-Rodríguez, J. Eur. Ceram. Soc., 24 (2004) 2793.
38 J. L. Perez-Rodriguez, A. Wiewiora, J. Drapala and L. A. Perez-Maqueda, Ultrasonics Sonochemistry, 13 (2006) 61.
39 L. A. Perez-Maqueda, F. Franco and J. L. Perez-Rodriguez, J. Eur. Ceram. Soc., 25 (2005) 1463.

DOI: 10.1007/s10973-007-8810-4